Molecular Biology of the Cell
Vol. 20, 995–1005, February 1, 2009

# ICAM-1–mediated Endothelial Nitric Oxide Synthase Activation via Calcium and AMP-activated Protein Kinase Is Required for Transendothelial Lymphocyte Migration

**Roberta Martinelli, Matthew Gegg, Rebecca Longbottom, Peter Adamson, Patric Turowski,* and John Greenwood***

Division of Cell Biology, Institute of Ophthalmology, University College London, London EC1V 9EL, United Kingdom

Submitted June 23, 2008; Revised October 20, 2008; Accepted December 3, 2008
Monitoring Editor: Martin A. Schwartz

**As a gatekeeper of leukocyte trafficking the vasculature fulfills an essential immune function. We have recently shown that paracellular transendothelial lymphocyte migration is controlled by intercellular adhesion molecule 1 (ICAM-1)-mediated vascular endothelial cadherin (VEC) phosphorylation [Turowski *et al.*, J. Cell Sci. *121*, 29–37 (2008)]. Here we show that endothelial nitric oxide synthase (eNOS) is a critical regulator of this pathway. ICAM-1 stimulated eNOS by a mechanism that was clearly distinct from that utilized by insulin. In particular, phosphorylation of eNOS on S1177 in response to ICAM-1 activation was regulated by src family protein kinase, rho GTPase, $Ca^{2+}$, CaMKK, and AMPK, but not Akt/PI3K. Functional neutralization of any component of this pathway or its downstream effector guanylyl cyclase significantly reduced lymphocyte diapedesis across the endothelial monolayer. In turn, activation of NO signaling promoted lymphocyte transmigration. The eNOS signaling pathway was required for T-cell transmigration across primary rat and human microvascular endothelial cells and also when shear flow was applied, suggesting that this pathway is ubiquitously used. These data reveal a novel and essential role of eNOS in basic immune function and provide a key link in the molecular network governing endothelial cell compliance to diapedesis.**

## INTRODUCTION

The events controlling the capture and subsequent migration of circulating lymphocytes across the vascular wall have been studied extensively, and many of its generic principles are known. However, the signaling mechanisms that underpin this process remain poorly defined. Endothelial cells (ECs) actively participate in directing and regulating the process of lymphocyte migration across the vascular wall via adhesion molecules such as vascular cell adhesion cell molecule 1 (VCAM-1; Engelhardt, 2006), platelet and endothelial cell adhesion molecule-1 (PECAM-1; Liao *et al.*, 1997), and intercellullar adhesion molecule 1 (ICAM-1; Turowski *et al.*, 2005). In the CNS, where ECs form a tight specialized barrier, lymphocyte recruitment utilizes the same adhesion molecules, with the pairing of lymphocyte function-associated antigen 1 (LFA-1)/ICAM-1 being preeminent in controlling diapedesis (Greenwood *et al.*, 1995; Turowski *et al.*, 2005).

Previous studies have also shown that ICAM-1 is not only involved in the adhesion process, but its engagement activates diverse signaling pathways in ECs, some of which are required for subsequent migration. For example, ICAM-1 has been reported to interact with members of the ezrin/radixin/moesin (ERM) family, to activate rho GTPases, src, protein kinase C (PKC), and mitogen-activated protein (MAP) kinases and a series of proteins involved in the formation of focal adhesions such as FAK, paxillin, and $p130^{cas}$ (Turowski *et al.*, 2005). A rise of intracellular calcium appears to be central to ICAM–mediated events (Etienne-Manneville *et al.*, 2000) and precedes the activation of the other master regulators such as rho GTPases and PKC. Importantly, EC signaling via $Ca^{2+}$ and rho is essential for subsequent lymphocyte migration (Adamson *et al.*, 1999; Etienne-Manneville *et al.*, 2000) at least in part by regulating adherens junction modulation during paracellular diapedesis (Allingham *et al.*, 2007; Turowski *et al.*, 2008). Indeed, ICAM-1 engagement induces phosphorylation of vascular endothelial cadherin (VEC) and concomitant paracellular permeability. This suggests that lymphocyte adhesion to ICAM-1 modulates the paracellular space much like vasoactive compounds such as vascular endothelial growth factor (VEGF) or histamine (Dejana *et al.*, 2008). A central mediator of VEGF or thrombin-induced endothelial permeability is nitric oxide (van Hinsbergh and van Nieuw Amerongen, 2002). Two nitric oxide synthase (NOS) systems are of physiological significance in ECs. Inducible NOS (iNOS) is regulated at the transcriptional level and is mainly utilized during long-term adaptation of the vasculature to extracel-

This article was published online ahead of print in *MBC in Press* (http://www.molbiolcell.org/cgi/doi/10.1091/mbc.E08–06–0636) on December 10, 2008.

* These authors contributed equally to this work.

Address correspondence to: John Greenwood (j.greenwood@ucl.ac.uk) or Patric Turowski (p.turowski@ucl.ac.uk).

Abbreviations used: EC, endothelial cell; ROS, reactive oxygen species; VEC, vascular endothelial cadherin; NO, nitric oxide; eNOS, endothelial nitric oxide synthase; XO, xanthine oxidase; NOX, NAPDH oxidase; AMPK, AMP-activated protein kinase; CaMKK, calcium/calmodulin kinase kinase; ICAM-1, intercellular adhesion molecule-1; VCAM-1, vascular cell adhesion molecule-1; L-NAME, $N^G$-nitro-L-arginine methyl ester; ODQ, 1H-[1,2,4]oxadiazole[4,3-a]quinoxalin-1-one.

lular cues. Endothelial NOS (eNOS) is constitutively expressed in the vasculature and in skeletal muscle, and its activity is highly regulated on many levels. For instance, caveolin-1, G-protein–coupled receptors (in particular bradykinin receptor 2 and the angiotensin II R1), and the eNOS-binding protein NOSIP bind to and inhibit eNOS activity (Fulton *et al.*, 2001).

Calmodulin and hsp90 have also been reported to stimulate eNOS activity (Pober and Sessa, 2007). Most importantly, eNOS activity has been shown to be modulated by phosphorylation on serine and threonine residues in response to a variety of agonists such as VEGF, insulin, and shear stress (Fulton *et al.*, 2001; Marletta, 2001). In particular, six residues, namely S116, T497, S617, S635, S1177, and Y83, have been identified as being phosphorylated during activation (Gallis *et al.*, 1999; Harris *et al.*, 2001; Fulton *et al.*, 2005). Phosphoinositide 3-kinase (PI3K) and Akt/PKB have been shown to be important regulators of eNOS both in vitro and in vivo (Dimmeler *et al.*, 1999; Fulton *et al.*, 1999; Six *et al.*, 2002). However, other pathways for eNOS activation are known. For example, thrombin-mediated eNOS activation depends on CaM kinase kinase (CaMKK) and AMP-activated protein kinase (AMPK; Stahmann *et al.*, 2006), and NO has been implicated in mediating some of the functions of AMPK (Morrow *et al.*, 2003; Nagata *et al.*, 2003).

The purpose of this study was to test whether eNOS was part of ICAM-1–mediated signaling in microvascular ECs. We also searched for upstream activators of eNOS. Finally, we analyzed whether ICAM-1–mediated paracellular regulation, including the compliance to lymphocyte diapedesis, was regulated by eNOS.

## MATERIALS AND METHODS

### *Materials*

Mouse mAbs to rat ICAM-1 (1A29 and 3H8) were generated from hybridomas provided by Dr. M. Miyasaka (Osaka University, Osaka, Japan) and Dr. W. Hickey (Dartmouth Medical School, Hanover, NH), respectively. Alternatively, low endotoxin IgG from Serotec (Oxford, United Kingdom) were used. Mouse mAb to human ICAM-1 (clone 15.2), rat CD11a (clone WT.1), and rat CD18 (clone WT.3) were also purchased from Serotec. Goat anti-mouse Abs (GAM) were from Sigma-Aldrich (Poole, United Kingdom). Polyclonal Ab specific for eNOS, Akt, AMPK, and their phosphorylated forms (eNOS Ser1177, AKT Ser 473, and AMPK Thr172) were from Cell Signaling Technology (Beverly, MA). Anti-CaMKK was purchased from BD Biosciences (Oxford, United Kingdom). Biotinylated anti-rabbit Ig and streptavidin-fluorescein were purchased from GE Healthcare (Amersham, United Kingdom). L-NAME ($N^G$-nitro-L-arginine methyl ester), ODQ (1H-[1,2,4]oxadiazolo-[4,3-a]quinoxalin-1-one), AICAR (5-aminoimidazole-4-carboxamide ribonucleoside), and BAPTA-AM were from Sigma-Aldrich. SU6656, wortmannin, LY294002, compound C, Akt1/2i, BAY-412272, and calyculin A were from Merck Biosciences (Nottingham, United Kingdom). STO-609 was from Tocris (Bristol, United Kingdom), and cell-permeable C3 transferase was from Cytoskeleton (Denver, CO). Phospho-specific peptide to eNOS IRTQ(pS)FSLQ and its control IRTQSFSLQ were from Genepep (Prades le Lez, France).

### *ECs and Endothelioma Lines*

The immortalized Lewis rat brain microvascular EC line GPNT and the mouse endothelioma cells bEnd5 and ICAM-1-deficient (bEndI1.1) were grown as previously described (Lyck et al., 2003; Romero et al., 2003). Primary cultures of cerebral ECs were prepared from 5–7-wk-old Lewis rats, 5–7-wk-old eNOS$^{-/-}$ mice (eNOS, F1 hybrid between SV129 and C57BLK/6, kindly provided by Dr. Adrian Hobbs, UCL, London) or wild-type mice, as previously described (Abbott *et al.*, 1992). Primary mouse and rat EC cells were seeded on collagen IV/fibronectin-coated plates and maintained in EGM-2 MV (Clonetics, Cambrex BioScience, Wokingham, United Kingdom). The primary dermal EC line, HDMEC-c (Promocell, Heidelberg, Germany), was also grown in EGM-2 MV medium.

### *Rho Activation Assay*

Cells were grown to confluence in 10-cm dishes. After appropriate stimulation, the cells were washed twice with ice-cold PBS and then lysed in 50 mM Tris buffer (pH 7.2), containing 500 mM NaCl, 10 mM $MgCl_2$, 1% Triton X-100, 1 mM DTT, and mixed protease inhibitors (Roche Diagnostics, Burgess Hill, United Kingdom). Each lysate was incubated with ca. 10 $\mu$g rhotekin rho-binding domain (Ren *et al.*, 1999) absorbed to glutathione beads at 4°C for 1 h. The beads were washed three times with lysis buffer and then processed for immunoblotting using monoclonal anti-rhoA antibody (Santa Cruz Biotechnology, Santa Cruz, CA).

### *Immunofluorescence*

Cells were grown to confluence in 35-mm dishes, stimulated, and fixed in 3.7% formaldehyde. After extraction in −20°C acetone, cells were processed for indirect immunocytochemistry. ICAM-1 distribution after incubation with mAb 1A29 was detected with anti-rat Cy3-conjugated antibody (1:50). Detection of phospho-eNOS was performed with phospho-specific antibodies (1:50), followed by biotinylated anti-rabbit Ig (1:100) and streptavidin-FITC (1:200). Where indicated, diluted primary antibody was preincubated with 10 $\mu$M eNOS-specific peptides IRTQ(pS)FSLQ or its nonphosphorylated control. Confocal microscopy was performed as previously described (Turowski *et al.*, 2004). For the analysis of ICAM-1 clustering confocal sections spanning the membrane area of cells and containing more than 90% of the ICAM-1 staining were stacked and quantified. The diameter of all fluorescent clusters (above the resolution limit of 0.2 $\mu$m) within an area of 25 $\mu m^2$ was measured using Zeiss LSM imaging software (Welwyn Garden City, United Kingdom).

### *Shear Stress*

Immortalized Lewis rat brain microvascular ECs (GPNT) were seeded in regular 12-well plates. Once confluent, cells were exposed to 10 dyn/cm of steady shear stress for 24 h on an orbital rotator as already described (Ley *et al.*, 1989).

### *T-cells*

For migration assays, myelin basic protein (MBP)-specific T lymphocyte lines were used (kind gift of Dr. E. Beraud, Marseille, France). Human whole blood was processed using Ficoll Paque to collect the peripheral blood mononuclear cells, following which T-cells were separated by positive selection using $CD4^+$ MACS beads (Miltenyi, Bisley, United Kingdom) according to the manufacturer's instructions. T-cells were cultured overnight at $1.5 \times 10^6$/ml in RPMI-1640 supplemented with 10% FCS, 100 U/ml penicillin, 100 $\mu$g/ml streptomycin,1 mM sodium pyruvate, 1 mM nonessential amino acids, 2 mM L-Glu, and 50 $\mu$m $\beta$-mercaptoethanol in the presence of recombinant IL-2 (50 U/ml).

### *Lymphocyte Migration In Vitro*

Lymphocyte migration assays on immortalized Lewis rat brain ECs (GPNT) were conducted as previously described (Adamson *et al.*, 1999). Rat T-cells were allowed to migrate for 30 min to 1 h at which point rates were determined by time-lapse video microscopy (see also Supplemental Videos). Migration of human T-cells across human dermal ECs was performed over course of 4 h. Migration data from static cultures was collected from triplicate experiments each representing a minimum of six wells. In shear stress experiments, rat T-cells were added to 12-well plates containing GPNT monolayers and incubated for 1.5 h at 37°C on an orbital rotator before recording by video microscopy. Added numbers from a minimum of four fields per assay were used.

### *Measurement of NO Production*

Cells were grown in 96-well plates and, at confluence, cultured in serum-free medium overnight. Medium from each well was removed and replaced with prewarmed phenol-red free HBSS containing the fluorescent dye 5 4,5-diaminofluorescein diacetate (DAF-2DA, Molecular Probes, Eugene, OR; 10 $\mu$M, 100 $\mu$l/well) for 120 min at 37°C for the detection of NO. After incubation, cells were washed twice with prewarmed HBSS before stimulation. The fluorescence of each well was measured in a fluorescence plate reader (excitation 490 nm, emission 520 nm). Results were obtained by subtracting the reading of controls from the correspondent reading for every time point after stimulation.

### *siRNA-mediated Knockdown of AMPK and CaMKK$\alpha$*

Specific siRNA duplexes targeting $\alpha$ subunits of AMPK, CaMKK$\alpha$, and non-silencing controls were purchased from Dharmacon (Chicago, IL). GPNT cells ($3 \times 10^5$) were seeded into six-well plates and transfected 24 h later with Oligofectamine Reagent following the manufacturer's instructions (Invitrogen, Paisley, United Kingdom). Briefly, 200 pmol siRNA was complexed with transfection reagent and added to the cells in serum-free medium for 4 h. Subsequently, serum was added, and the incubation proceeded for 24 h before repeating the transfection with siRNA. Cells were cultured for a further 48 h before experiments were performed.

### *Immunoprecipitation and Western Blotting*

Cells were seeded at $1 \times 10^5$/ml and, at confluence, cultured in serum-free medium overnight. Cells were pretreated and stimulated as detailed in the

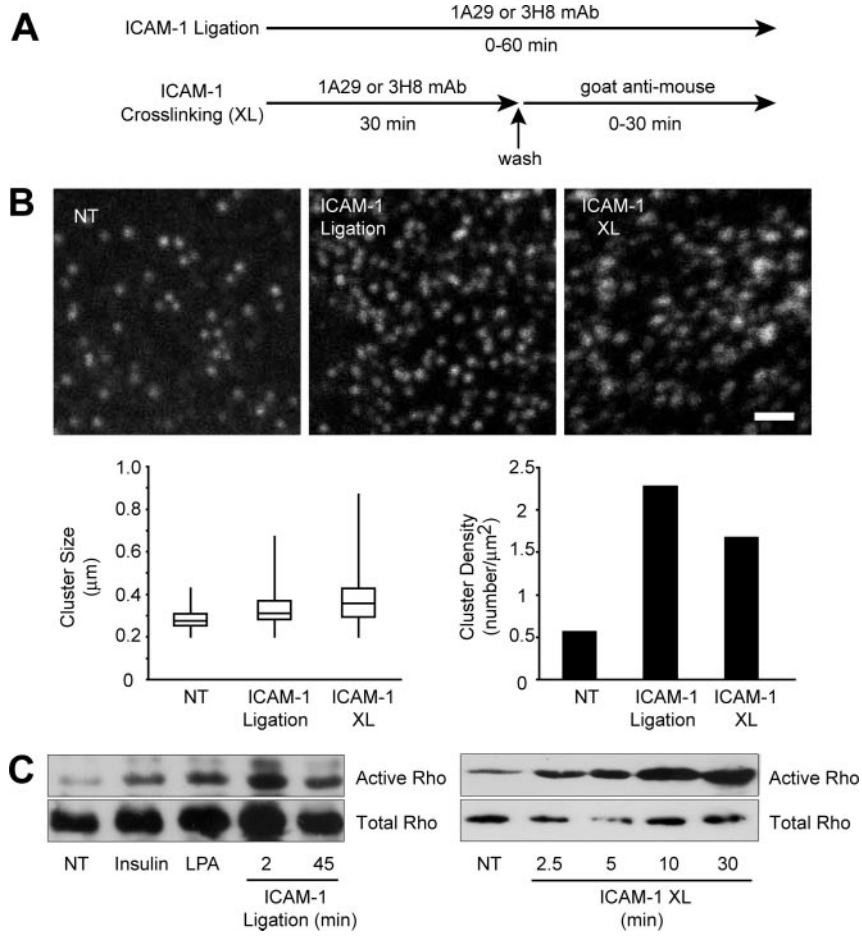


**Figure 1.** ICAM-1–mediated endothelial signaling. (A) Schematic representation of strategies used to activate ICAM-1 on ECs. (B) Antibody-induced ICAM-1 surface clustering. Confluent, serum-starved GPNT cells were either left untreated (NT) or incubated with 10 $\mu$g/ml ICAM-1 antibody 1A29 for 60 min (ICAM-1 ligation). Alternatively, at 30 min cells were briefly washed, and receptor cross-linking was induced by the addition of 10 $\mu$g/ml goat anti-mouse IgG for 30 min (XL). Cells were fixed and stained for ICAM-1 and analyzed by confocal microscopy. Cluster size was determined as described in *Materials and Methods* in at least 20 random areas, and their size distribution is represented in box plots. Average cluster density in these areas is represented on the right. Data are representative of three independent experiments. Bar, 1 $\mu$m. (C) Confluent, serum-starved GPNT cells were either left untreated or incubated with insulin (1 $\mu$M, 15 min), lysophosphatidic acid (LPA, 10 $\mu$M, 15 min), or ICAM-1 antibody 1A29 (10 $\mu$g/ml) for the times indicated (left). Alternatively, at 30 min, cells were briefly washed and receptor cross-linking induced by the addition of 10 $\mu$g/ml goat anti-mouse IgG for the indicated times (right). Cells were then lysed, and the amount of activated (top) and total rho GTPase (bottom) was determined by pulldown assays. Similar results were obtained in at least three independent experiments.

figure legends and then lysed in boiling 50 mM Tris/Cl, pH 6.8, 2% SDS, 10% glycerol, 100 mM DTT, 100 nM calyculin A (200 $\mu$l/60-mm dish). Immunoprecipitation of VEC was performed as previously described (Turowski *et al.*, 2008). Samples were subjected to SDS-PAGE and transferred to nitrocellulose by semidry electrotransfer. The membranes were blocked in TBS containing 5% milk, 0.1% Tween-20, and 0.1% Triton X-100 for 2 h before incubation overnight at 4°C with the appropriate antibody diluted at 1:1000 in TBS containing 0.1% Tween-20 and 0.1% Triton X-100. Membranes were washed three times with PBS/0.1% Tween-20 before 1-h incubation with an anti-mouse or anti-rabbit HRP-conjugated IgG (GE Healthcare) at a dilution of 1:10,000 and 1:2000, respectively. After three washes in PBS/0.1% Tween-20, membranes were developed using the ECL reagents (Roche) according to the manufacturer's instructions and exposed to x-ray film. Protein bands were evaluated by densitometric quantification, normalized against the amount of total protein, and averaged over at least three independent experiments.

### *Statistical Analyses*

Data are presented as mean ± SEM. Variances of mean values were statistically analyzed by the Student's *t* test. *$p < 0.05$; **$0.001 < p < 0.01$; ***$p \leq 0.001$. Time-course data were analyzed by linear regression, and the significance of slopes was determined by analyses of covariance (ANCOVA) using the Prism software package.

## RESULTS

LFA1–ICAM-1 clustering plays a fundamental role during leukocyte transmigration (Barreiro *et al.*, 2002, Carman *et al.*, 2003). Subsequent endothelial ICAM-1 signaling involves $Ca^{2+}$, rho GTPases, protein kinases, and actin rearrangements and has generally been studied by antibody-mediated cross-linking of serum-starved cells (Turowski *et al.*, 2005). Specifically, experimental protocols usually involve incubation of cells with a primary anti-ICAM-1 antibody for 5–30 min (believed to be a neutral period), followed by clustering using secondary antibody that triggers the cellular signaling response (Figure 1A). This was illustrated by a loss of signaling to actin when ICAM-1 clustering was prevented (Supplemental Figure S1A). Additionally, we have found that a variety of monoclonal primary anti-ICAM-1 antibodies on their own, i.e., not followed by cross-linking with a secondary Ab, induced ICAM-1 signaling in ECs, exemplified by receptor surface clustering (Figure 1B), rho GTPase activation (Figure 1C), $Ca^{2+}$ transients (Supplemental Figure S1B), and VEC phosphorylation (see Figure 3C). This indicated that ICAM-1–mediated signaling was activated using primary antibody alone and suggested that certain immediate early signals such as oscillating $Ca^{2+}$ (Supplemental Figure S1B) or NO production (see below) may have previously been overlooked. In the following, all EC activation was performed by either anti-ICAM-1 antibody alone or T-cells.

### *ICAM-1 Induces eNOS Phosphorylation*

eNOS activation was determined by measuring phosphorylation of S1177 (Harris *et al.*, 2001). Primary rat cerebral microvascular ECs were stimulated with 1A29 mAb for various times and the level of activated eNOS determined in Western blots using anti-phospho S1177 eNOS antibodies (Figure 2A). ICAM-1 ligation induced strong phosphorylation of eNOS within 15 min. Positive control cells, stimulated with insulin (Montagnani *et al.*, 2001; Fleming *et al.*,

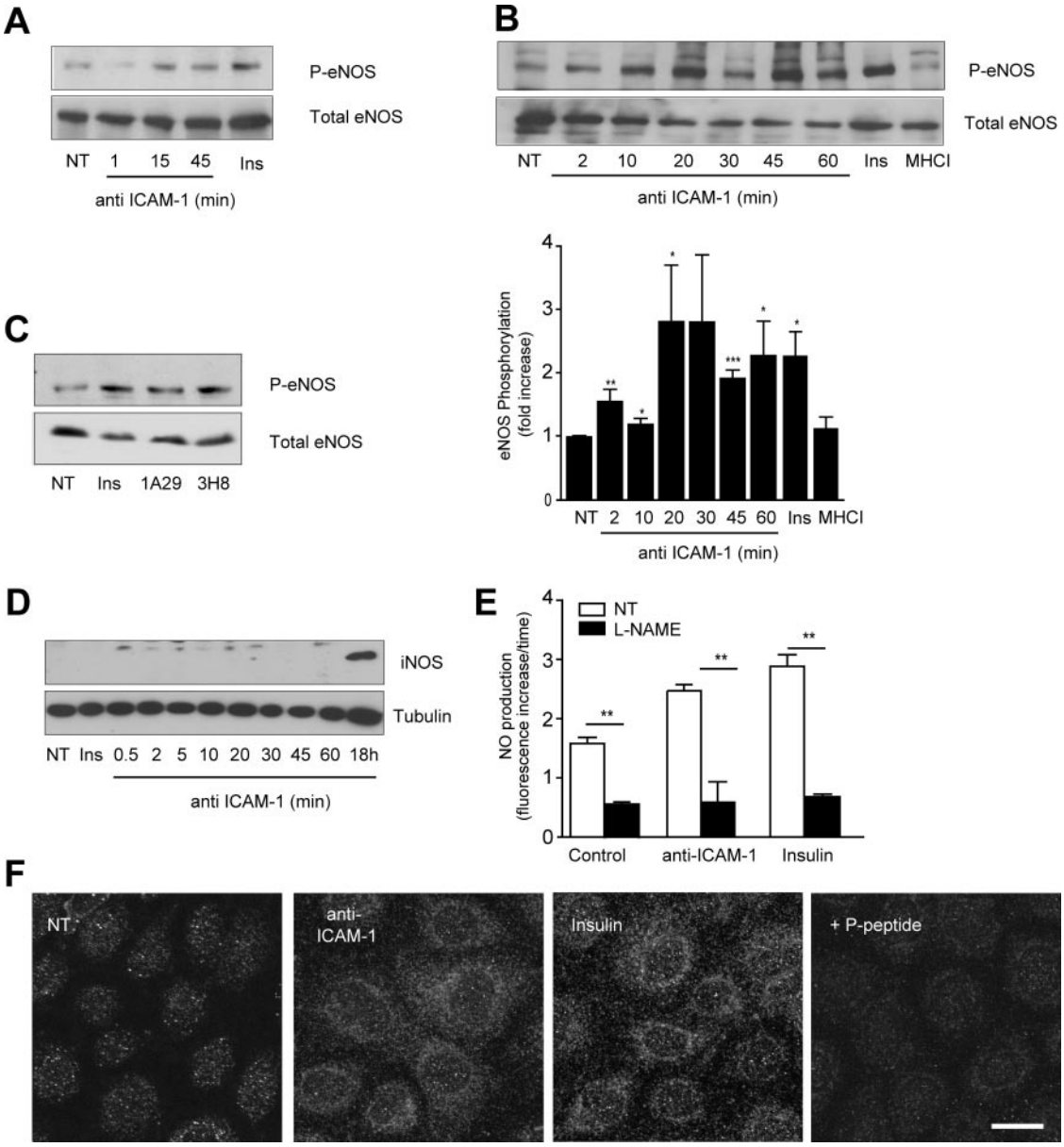


**Figure 2.** ICAM-1 engagement induces phosphorylation of eNOS in ECs. (A) Primary brain microvascular ECs were either left untreated (NT) or treated with insulin (1 $\mu$M, 15 min) or 1A29 (10 $\mu$g/ml) for the indicated times. Total protein extracts (ca. 50 $\mu$g) were analyzed by immunoblotting with anti-phospho-S1177 eNOS antibodies. The blot was subsequently stripped and probed for total eNOS. (B) As in A, except that GPNT brain microvascular ECs were used. Densitometric quantification (means ± SEM) of three independent experiments is shown in the bottom panel. (C) As in B, except that GPNT cells were treated with insulin (1 $\mu$M, 15 min), 1A29 (10 $\mu$g/ml), and anti-ICAM-1 3H8 (10 $\mu$g/ml, 20 min). (D) As in B, except that extract were immunoblotted for iNOS or tubulin. (E) Measurement of NO production using DAF-2A. GPNT cells were stimulated by adding either anti-ICAM-1 mAb 1A29 (10 $\mu$g/ml) or insulin (Ins, 1 $\mu$M). Where indicated, GPNT cells were pretreated with L-NAME (600 $\mu$M, 1 h). The oxidization of DAF-2DA was then measured over the course of a linear 30-min period (Supplemental Figure S2D). Shown are rates of NO accumulation as derived by linear regression. The response to 1A29 or insulin was very significant ($p < 0.001$), whereas reduction in response to L-NAME was extremely significant ($p < 0.00001$) as calculated by ANCOVA. (F) GPNT cells were either left untreated (control) or treated with insulin (1 $\mu$M, 15 min) or anti-ICAM-1 mAb (10 $\mu$g/ml) for 20 min. Subsequently, cells were fixed and stained for phospho-eNOS. Where indicated, the immunogenic peptide was added to compete for antibody binding. Bar, 10 $\mu$m.

2003), also displayed increased eNOS phosphorylation (Figures 2A, 3B, 4B, and 5C). More detailed time-resolved analysis was performed in the GPNT EC line. Phosphorylation of eNOS rose significantly within 2 min of ICAM-1 ligation, reached maximal (ca. threefold increase) levels after 20–30 min, and persisted for at least another 60 min (Figure 2B). This effect was specific to ICAM-1 activation, because the addition of an antibody directed to MHC class I did not affect the phosphorylation of eNOS (Figure 2B). In contrast two mAb specific to ICAM-1 and used throughout this study, namely 1A29 and 3H8, produced a similar activation of eNOS (Figure 2C). iNOS was not expressed within 1 h of ICAM-1 stimulation (Figure 2D), which suggested that it was not relevant in our experimental setup. Significantly,

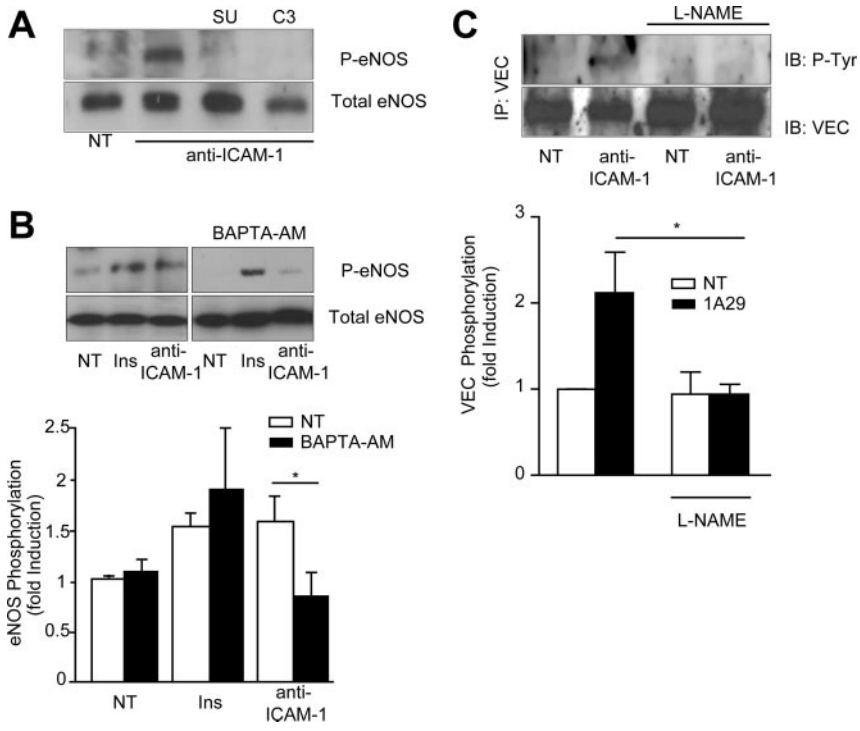


**Figure 3.** ICAM-1-induced VEC phosphorylation is mediated by eNOS. (A) GPNT cells were either left untreated (NT) or pretreated with SU6656 (10 $\mu$M, 1 h) or cell-permeable C3 transferase (3.75 $\mu$g/ml, 2 h) before ICAM-1 stimulation (45 min) and immunoblot analysis of phosphorylated and total eNOS. (B) Where indicated, GPNT cells were pretreated with BAPTA-AM (20 $\mu$M, 30 min) before analysis (performed as in A). Densitometric quantification (means ± SEM) of three independent experiments is shown below. (C) GPNT cells were pretreated with 1 mM L-NAME or left untreated before stimulation with anti-ICAM-1 mAb (10 $\mu$g/ml) for 15 min. VEC was then immunoprecipitated and its tyrosine phosphorylation analyzed with the phosphospecific antibody 4G10. A representative figure and densitometric quantification (means ± SEM) of three independent experiments is shown.

increased phosphorylation of eNOS correlated with an increase of NO. As reported by others (Matheny *et al.*, 2000), the adhesion of lymphocytes to GPNT induced reactive oxygen species (ROS) in the ECs (Supplemental Figure S2). Unlike in other EC systems, ROS accumulation in GPNT cells was largely dependent on ICAM-1 and specifically abolished by the NOS inhibitor L-NAME. This suggested that these ROS were in fact reactive nitrogen species, and this was tested directly in GPNT loaded with DAF-2DA, a dye that fluoresces upon binding to oxidized species of NO. Stimulation with 1A29 or insulin induced a time-dependent, linear increase in DAF-2DA fluorescence (Supplemental Figure S2D) at a significantly higher rate than nonstimulated control cells (Figure 2E). Changes in DAF-2DA fluorescence were sensitive to L-NAME pretreatment suggesting they were due to eNOS activity (Figure 2E). Detailed subcellular analysis of the distribution of activated eNOS was performed using anti-phospho eNOS antibodies in indirect immunofluorescence (Figure 2F). Insulin and ICAM-1 activation induced a similar increase in phospho-eNOS staining in GPNT cells. In both cases specific staining was punctate, suggesting vesicular eNOS association, and was enriched in pericellular areas of the cell. Collectively, these data suggested that endothelial ICAM-1 stimulation induced eNOS and the production of oxygen species, among which NO and/or oxidized derivatives constituted the vast majority.

### *ICAM-1 and Insulin Activate eNOS by Different Signal Transduction Pathways*

Endothelial signaling after ICAM-1 stimulation is controlled by src protein kinases (Etienne-Manneville *et al.*, 2000; Wang *et al.*, 2003) and rho GTPase (Etienne *et al.*, 1998; Adamson *et al.*, 1999). Pharmacological inhibition of these major signal transducers abolished ICAM-1–induced activation of eNOS (Figure 3A). $Ca^{2+}$ is a critical mediator of ICAM-1 signaling (Etienne-Manneville *et al.*, 2000; Supplemental Figure S1B) and has also been implicated in the activation of eNOS (Busse and Mulsch, 1990). We therefore tested whether $Ca^{2+}$ was also involved in ICAM-1– or insulin-mediated eNOS activation. Intracellular $Ca^{2+}$ was chelated using BAPTA-AM, and subsequently eNOS phosphorylation was assessed (Figure 3B). Depletion of $Ca^{2+}$ did not affect insulin-induced eNOS phosphorylation, in line with previous observations (Montagnani *et al.*, 2001). By contrast, ICAM-1–induced eNOS activation was reduced to basal levels in BAPTA-AM–pretreated cells. These data implicated $Ca^{2+}$, rho GTPases, and src protein kinases upstream of eNOS activation in response to ICAM-1 activation. Endothelial ICAM-1 signaling regulates a variety of processes ranging from focal adhesion to transcription. However, among these, only modulation of intercellular junctions through VEC phosphorylation has so far been shown to be relevant to leukocyte migration (Turowski *et al.*, 2008). We tested whether ICAM-1 engagement mediated phosphorylation of VEC via a pathway involving eNOS. ICAM-1 activation led to an ~2.5-fold increase in VEC tyrosine phosphorylation (Figure 3C). In cell pretreated with L-NAME, the ICAM-1–induced phosphorylation was totally absent. Significantly, insulin did not induce any phosphorylation of VEC (data not shown), further underlining that insulin and ICAM-1 engaged separate signaling pathways in microvascular ECs.

### *ICAM-1 Induces eNOS Activation via AMPK*

Akt/PKB has been shown to directly activate eNOS in ECs in response to VEGF or insulin (Dimmeler *et al.*, 1999; Hill *et al.*, 2001). Phospho-Akt could be detected in insulin-stimulated GPNT cells but not in response to the ligation of ICAM-1 (Figure 4A). This inability of ICAM-1 to activate Akt/PKB was expected because, at least in B-cells, this is a prerogative of ICAM-2 (Perez *et al.*, 2002). Inhibition of PI3K by wortmannin obliterated insulin-induced eNOS activation but left the response to ICAM-1 intact (Figure 4B), further supporting that insulin and ICAM-1 signaling engage separate pathways in brain microvascular ECs. In search of a

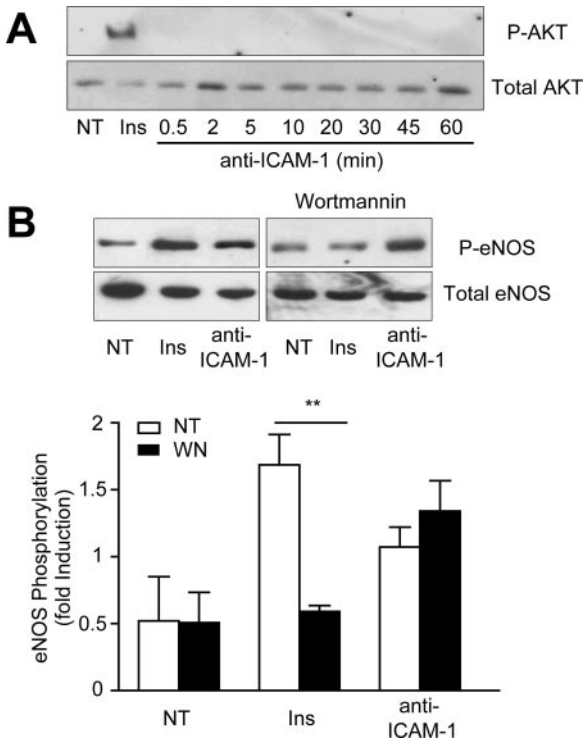


**Figure 4.** ICAM-1–induced eNOS activation is independent of PKB/Akt. (A) GPNT cells were either left untreated (NT), treated with insulin (1 $\mu$M, 15 min) or anti-ICAM-1 mAb (10 $\mu$g/ml) for the indicated times. Total protein extracts (ca. 50 $\mu$g) were analyzed by immunoblotting using anti-phospho-T493 and total Akt antibodies. (B) GPNT cells were treated with insulin (1 $\mu$M, 15 min) or anti-ICAM-1 mAb (10 $\mu$g/ml, 45 min). Where indicated, cells were pretreated with wortmannin (WN, 20 $\mu$M, 30 min). eNOS activation was analyzed and quantified as in Figure 2.

mediator of ICAM-1–induced eNOS activation we turned to AMPK, which can also phosphorylate eNOS S1177 (Morrow *et al.*, 2003; Nagata *et al.*, 2003). To investigate whether AMPK was involved in ICAM-1–dependent signaling in rat microvascular ECs, kinase phosphorylation was monitored using specific antibodies. Rapid and transient phosphorylation of AMPK at Thr172 was detected in response to ICAM-1 stimulation, with a distinct peak at 0.5 min and a return to control levels within 20 min (Figure 5A). Similar phosphorylation of endothelial AMPK was obtained when T-cells were added (Figure 5B). Phosphorylation was sensitive to pretreatment with inhibitors targeting src protein kinases or rho GTPase, placing AMPK downstream of this well-established axis of ICAM-1 signaling (Figure 5C). Next, we investigated whether AMPK was required for ICAM-1–induced eNOS activation. For this, GPNT were pretreated using compound C, a selective inhibitor of AMPK (Zhou *et al.*, 2001). Significant reduction in the phosphorylation of eNOS was detected, indicating that AMPK was instrumental to ICAM-1–induced eNOS stimulation (Figure 5D). In contrast, insulin-induced eNOS phosphorylation was insensitive to compound C, again underlining the molecular differences in signaling. The involvement of AMPK in ICAM-1–mediated eNOS phosphorylation was further corroborated by siRNA-mediated knockdown. Transfection of GPNT cells with siRNA complexes specifically targeting AMPK led to nearly 50% reduction in protein levels (Figure 5E). Cells with reduced levels of AMPK displayed somewhat higher phosphorylation of eNOS, but this was completely abolished in response to ICAM-1 (Figure 5F). Because calcium plays an important role in ICAM-1–mediated signaling (Supplemental Figure S1B) and AMPK can be activated by the calcium-dependent CaMKK (Hurley *et al.*, 2005), we investigated whether this kinase was relevant in our system. siRNA-mediated knockdown targeting CaMKK led to a 40% reduction in protein levels (Figure 5E). Under these conditions eNOS phosphorylation was also significantly reduced in response to ICAM-1 stimulation (Figure 5F). These results revealed that VEC phosphorylation is linked to ICAM-1 activation via $Ca^{2+}$, CaMKK, AMPK, and eNOS.

### *Lymphocyte Diapedesis Requires eNOS Signaling*

Finally, we investigated whether eNOS signaling was also required for leukocyte transmigration. For this, we used a well-documented in vitro system of an antigen activated T-cell line cocultured with primary or established brain microvascular ECs (Adamson *et al.*, 1999). T-cell transmigration is monitored by time-lapse video microscopy and importantly, occurs in the absence of cytokine stimulation or chemokine gradients (see also Supplemental Videos). Transmigration is strongly dependent on ICAM-1 (Greenwood *et al.*, 1995). Specifically, we observed more than 60% reduction of T-cell migration across GPNT monolayers when LFA-1 was blocked beforehand (Figure 6A). L-NAME pretreatment of GPNT cells induced a similar block in migration, as did the inhibition of the NO effector soluble guanylyl cyclase (sGC) using ODQ (Figure 6B). In sharp contrast, inhibition of other important intracellular oxidase systems such as xanthine oxidase (XO) and NADPH oxidase (NOX) had no effect on migration rates (Supplemental Figure S3). L-NAME did not affect lymphocyte migration across primary brain ECs derived from $eNOS^{-/-}$ mice, indicating that this NOS inhibitor has no other relevant intracellular target (Supplemental Figure S4A). Exogenous addition of the NO donor DEA-NO to cocultures led to a modest increase in T-cell migration but potently reversed a block exerted by BAPTA-AM (Figure 6B). Chelating endothelial $Ca^{2+}$ is one of the most effective ways of inhibiting leukocyte migration (Etienne-Manneville *et al.*, 2000), and this blockade was completely reversed when ECs were pretreated with DEA-NO or when the sGC agonist BAY-412272 was added during migration. However, inhibition of migration through ODQ could not be reversed by addition of exogenous NO (Figure 6B), indicating that NO was required downstream of $Ca^{2+}$ and upstream of sGC signaling. Significantly, in all cases, inhibition of migration was due to reduced diapedesis because lymphocyte adhesion to ECs was unchanged (Supplemental Figure S5). Thus eNOS and NO played an integral part of ICAM-1–dependent lymphocyte migration across GPNT cells. To further confirm the importance of eNOS signaling we tested the upstream regulators. Inhibition of endothelial PI3K or Akt did not affect lymphocyte transmigration, confirming that this pathway is not relevant for ICAM-1 signaling (Figure 6C). In clear contrast the pharmacological inhibition of either AMPK or CaMKK led to a reduction in migrated lymphocytes similar to that observed when ICAM-1 engagement or NOS was blocked (Figure 6D). This effect was specific because siRNA-mediated knockdown of these kinases also significantly reduced transmigration (Figure 6D). The effect of L-NAME was not only restricted to the GPNT cell line. Migration across primary rat cerebral or human dermal microvascular ECs was also inhibited in response to L-NAME or compound C treatment (Figure 7,A–C). Shear flow is an important parameter in all processes of the vascular endothelium. T-cell migration across GPNT was also assessed after exposure to shear stress (Figure 7, D

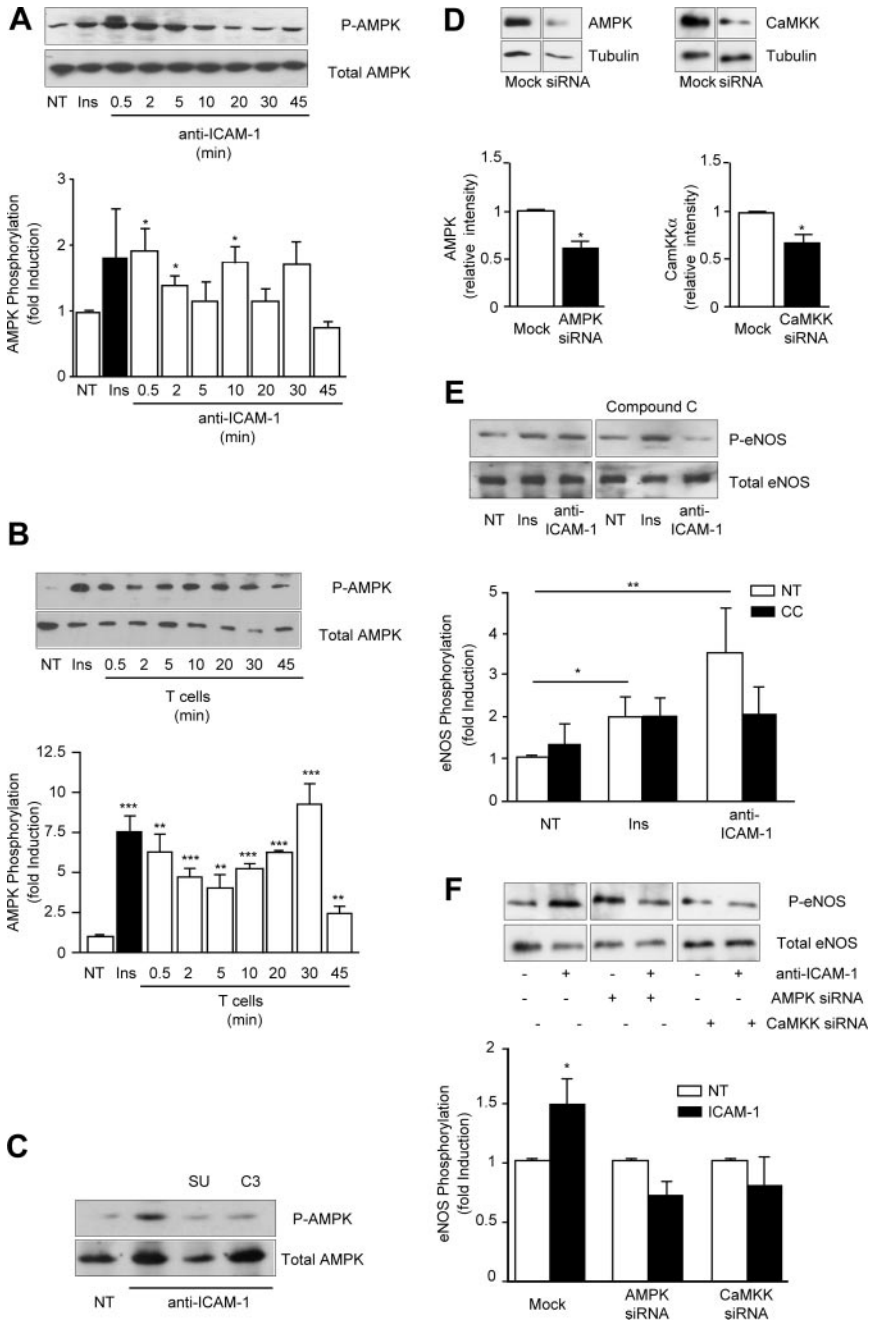


**Figure 5.** ICAM-1–induced eNOS activation is dependent on AMPK and CaMKK. (A and B) GPNT cells were either left untreated (NT), treated with insulin (1 $\mu$M, 15 min) or anti-ICAM-1 mAb (10 $\mu$g/ml; A), or incubated in the presence of T-cells (ca. five T-cells/EC; B) for the indicated times. Total protein extracts (ca. 50 $\mu$g) were analyzed by immunoblotting using anti-phospho-T172 and total AMPK antibodies and quantified as described for Figure 2. (C) Where indicated, cells were pretreated with SU6656 (10 $\mu$M, 1 h) or C3 transferase (3.75 $\mu$g/ml, 2 h) before ICAM-1 stimulation (5 min) and immunoblot analysis of phospho-AMPK (performed as for A). (D) GPNT cells were either left untreated or pretreated with compound C (CC, 20 $\mu$M, 30 min) before stimulation either with insulin (1 $\mu$M, 15 min) or anti-ICAM-1 mAb (10 $\mu$g/ml, 45 min). Total and phospho-eNOS levels were determined by immunoblotting. (E) AMPK or CaMKK in GPNT were knocked down using siRNA as described in *Materials and Methods.* After 72 h the remaining levels of these kinases were determined and correlated to tubulin levels by immunoblot analyses. The histograms below show the average knockdown achieved over three independent experiments. (F) AMPK or CaMKK were knocked down as described in E. Subsequently, ICAM-1–induced eNOS phosphorylation was determined in immunoblots as described in D (top panel). Densitometric quantification (means ± SEM) from three independent experiments is shown below.

and E). Again, both L-NAME and compound C significantly inhibited T-cell migration to an extent similar to that observed for static conditions, suggesting that eNOS controlled diapedesis under physiological conditions.

## DISCUSSION

ICAM-1 has been shown to modulate a variety of intracellular signaling pathways and its importance in regulating leukocyte migration across the endothelium has been well documented (Turowski *et al.*, 2005). In particular, its activation induces adherens junction modulation through tyrosine phosphorylation of VEC and thus facilitates paracellular passage of transmigrating leukocytes (Allingham *et al.*, 2007; Turowski *et al.*, 2008). Here we show that endothelial NOS is an important link in this process.

Significant effects on NOS were only observed when ICAM-1 was activated with primary antibodies alone. Subsequent cross-linking did not alter NO levels or eNOS phosphorylation (data not shown). We also provide evidence that divalent anti-ICAM-1 antibodies induced clustering of ICAM-1, suggesting that ICAM-1 is organized in membrane nanodomains similar to those reported for LFA-1 (Cambi *et al.*, 2006). This clustering effect of anti-ICAM-1 antibodies alone and ensuing signaling events may have previously been overlooked because investigators have focused on time points after addition of secondary, "clustering" antibodies. Importantly, increased NOS activity was not only observed

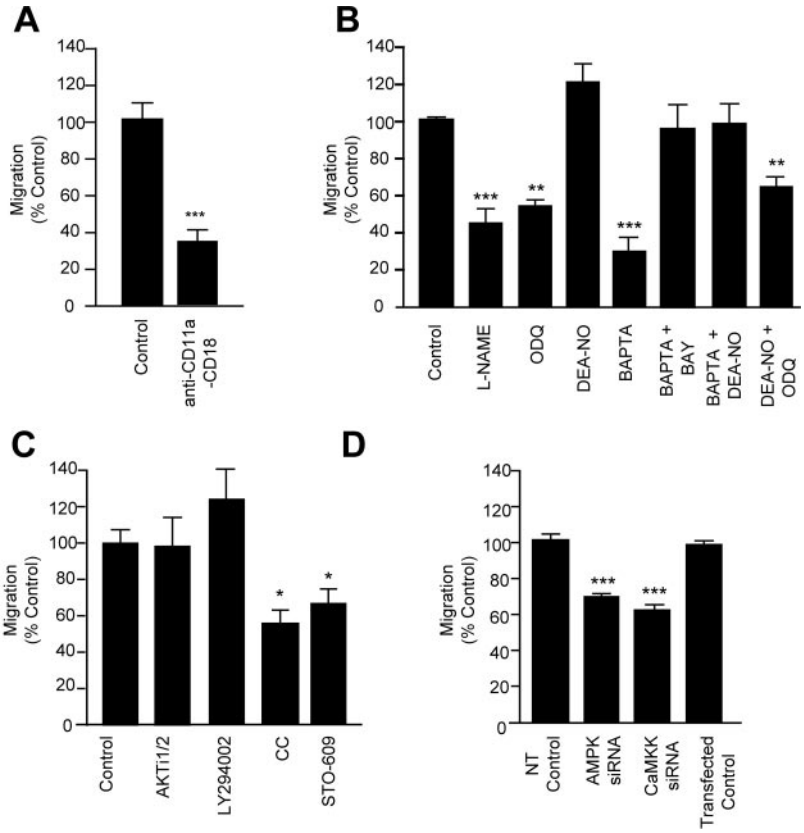


**Figure 6.** Signaling pathways required for transendothelial lymphocyte migration. (A) Contribution of ICAM-1 to T-cell migration. T-cells were either left untreated or preincubated with antibodies against CD11a (10 $\mu$g/ml) and CD18 (10 $\mu$g/ml) for 1 h before assessing migration across GPNT cells monolayers. (B) GPNT cells were left untreated (Control) or treated with various pharmacological inhibitors, alone or in combination, before migration. ECs were pretreated with L-NAME (600 $\mu$M) or ODQ (100 $\mu$M) for 1 h or BAPTA-AM (20 $\mu$M) for 30 min before migration. Alternatively cells were stimulated with DEA-NO (5 $\mu$M) for 30 min before lymphocyte migration assays. The sGC agonist BAY 41–2272 (50 $\mu$M) were added for 30 min before and kept throughout the lymphocyte migration assays. (C) Migration assay similar to B. GPNT cells were pretreated with the Akt inhibitor Akti1/2 (2.5 $\mu$M, 30 min), the PI3-kinase inhibitor LY294002 (20 $\mu$M, 1 h), the AMPK inhibitor compound C (20 $\mu$M, 30 min), or the CaMKK inhibitor STO-609 (10 $\mu$M, 1 h) before migration. (D) GPNT cells were transfected with siRNA targeting CaMKK$\alpha$ or AMPK 72 h before the migration assay. All results are the mean $\pm$ SEM of six replicates from at least three independent experiments.

in response to antibody-mediated clustering but also during lymphocytes adhesion (Supplemental Figure S2).

At times that appeared relevant to transendothelial lymphocyte migration we observed a time-dependent phosphorylation of eNOS on S1177, an activation site in the reductase domain of the enzyme (Fulton *et al.*, 2001). A corroborative rise in intracellular concentration of reactive nitrogen species was also detected, both in response to ICAM-1 ligation and insulin. Reactive nitrogen species were measured in cells loaded with DAF-2DA, a dye that fluoresces upon binding to a variety of oxidized species of NO. They are likely to represent NO because inhibition of the intracellular NO receptor sGC displayed effects similar to that of NOS inhibition. Significant eNOS phosphorylation was subcellularly restricted to vesicular structures, suggesting that ICAM-1–induced nitrogen oxide species affected signaling locally.

The phosphorylation of at least five S/T residues plays a role in the activation of eNOS and PKB/Akt has been identified as a critical activator in many situations (Fulton *et al.*, 1999; Montagnani *et al.*, 2001). When eNOS was activated in response to ICAM-1, PKB/Akt clearly did not play a role. First, ICAM-1 failed to induce PKB/Akt phosphorylation in agreement with a previous report (Perez *et al.*, 2002). Second, neither PI3K nor Akt inhibitors affected ICAM-1–induced phosphorylation or ICAM-1–dependent lymphocyte migration. There is precedence of Akt-independent activation of eNOS, exemplified by stimulation of human umbilical venous endothelial cells (HUVECs) with fenofibrate (Murakami *et al.*, 2006) or when bovine aortic ECs are exposed to shear stress (Boo *et al.*, 2002) or thrombin (Motley *et al.*, 2007). Although we were unable to demonstrate an involvement of PI3K or PKB/Akt, a role for AMPK was clearly shown. This protein kinase is an energy-sensing enzyme that has been reported to mediate a number of metabolic signals such as inhibition of cholesterol, fatty acid and protein synthesis, and enhancement of glucose uptake and blood flow

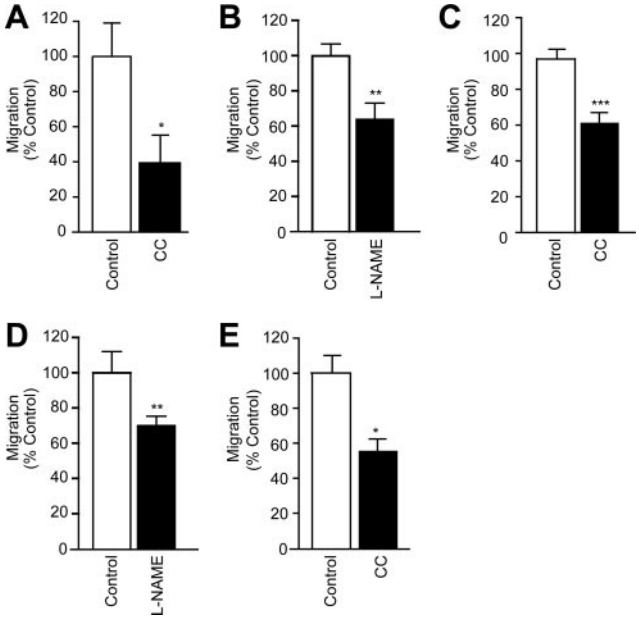


**Figure 7.** eNOS signaling is required for T-cell migration across a variety of ECs. (A) T-cell migration assay similar to Figure 6, except that primary rat brain ECs were used. (B and C) T-cell migration assay similar to Figure 6, except that human primary dermal cells were used. (D and E) The effect of L-NAME and compound C on migration across GPNT cells was assessed when shear stress was operational.

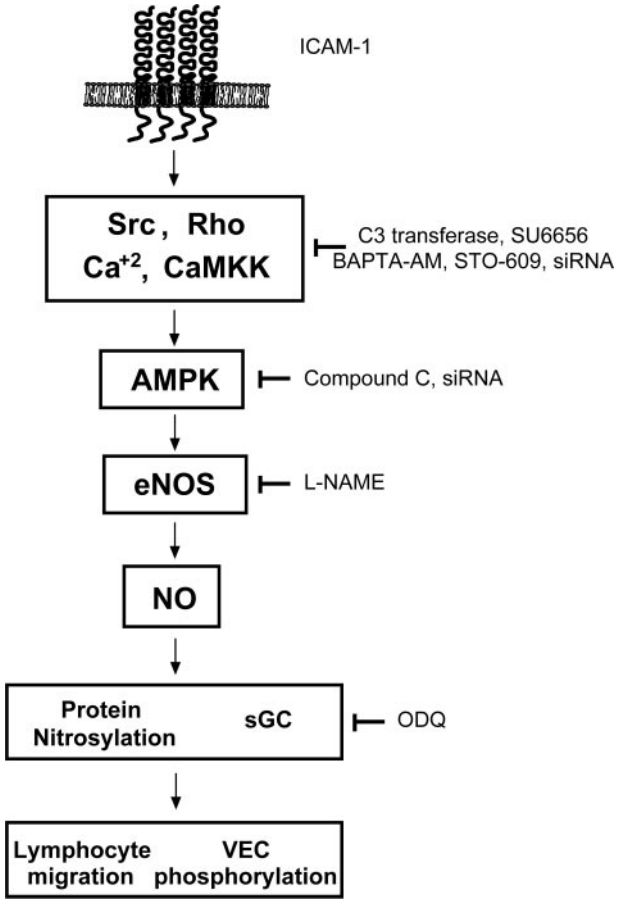


**Figure 8.** Schematic representations of events after ICAM-1–induced activation on brain microvascular ECs. See *Discussion* for additional details.

(Hardie *et al.,* 2006). Many reports also implicate AMPK in the activation of eNOS, possibly by directly phosphorylating S1177 (Chen *et al.,* 1999; Fleming *et al.,* 2003; Morrow *et al.,* 2003; Nagata *et al.,* 2003), and our data suggested this to be the case in response to endothelial ICAM-1 activation as well. Consistent with a potential upstream role, phosphorylation of AMPK preceded that of eNOS. Furthermore, pharmacological inhibition (using compound C) or functional neutralization (using siRNA) of AMPK prevented ICAM-1–induced eNOS activation. AMPK activation could be placed downstream of src protein kinase, rho GTPase and CaMKK, the latter presumably providing a link to ICAM-1–induced $Ca^{2+}$ signaling. Collectively and as summarized in Figure 8, our data identified CaMKK, AMPK, and eNOS as mediators of ICAM-1–induced endothelial junction modulation.

Both insulin- and ICAM-1–induced similar S1177 phosphorylation of eNOS in brain microvascular ECs, but the signaling network and the molecular outcome were clearly distinct. In contrast to the ICAM-1 pathway, insulin induced eNOS via PI3K and PKB/Akt, also demonstrating that this pathway is relevant in our cell system. Furthermore, insulin led to the activation of AMPK, but this was not functionally linked to that of eNOS. Therefore distinct spatiotemporal networks were operational, and this was further underlined by our observation that VEC phosphorylation was unchanged in the presence of insulin (data not shown). Indeed, insulin has also been shown to phosphorylate eNOS on Y657 (Fisslthaler *et al.,* 2008), which may be how it exerts its well-documented role in protecting endothelial barrier function (van Hinsbergh and van Nieuw Amerongen, 2002). Taken together, ICAM-1–induced signaling was clearly different and as hypothesized at the outset of this study, comparable to that induced by other proinflammatory or vasogenic stimuli such as thrombin (Stahmann *et al.,* 2006).

Significantly, every component of the newly identified endothelial ICAM-1 signaling pathway was shown to be required for lymphocyte migration. In our simple two-cell coculture system, diapedesis of antigen activated T-cells was predominantly dependent on LFA-1 interacting with and activating endothelial ICAM-1 (Figure 6A). We have performed our analyses in the absence of inflammatory cues so that migration was independent of VCAM-1 (Matheny *et al.,* 2000), the signaling of which additionally involves reactive oxygen synthase systems other than NOS (Cook-Mills, 2002; Deem and Cook-Mills, 2004). In our system, BAPTA-AM affected lymphocyte migration more potently than LFA-1 blockade alone, presumably because it also affected G protein–coupled receptor-dependent signaling (unpublished observations), which also plays an important role (Adamson *et al.,* 2002). Inhibition or functional neutralization of CaMKK, AMPK, eNOS, or sGC reduced lymphocyte migration on average by 40–50%, which constituted ca. 80% of what could be achieved using anti-LFA-1 antibodies. In light of the reversible nature of most of the inhibitors used and the only partial knockdown using siRNA (to preserve EC integrity), these numbers suggested that the identified components were mediators of ICAM-1–mediated compliance to lymphocyte migration. Cells with reduced levels of eNOS were not used because the prolonged absence of eNOS appeared to induce pleiotropic effects. For instance migration of lymphocytes across ECs from $eNOS^{-/-}$ mice was significantly up-regulated (Supplemental Figure S4A), presumably because of increased adhesion molecule expression (Ahluwalia *et al.,* 2004). Nevertheless, migration of lymphocytes across ECs lacking eNOS was unaffected by L-NAME, validating eNOS as its sole target in our experimental setup (Supplemental Figure S4B).

The role of endothelial NO during lymphocyte diapedesis is not clearly defined. Although many reports show that NO inhibits migration, possibly through reduction in the expression of adhesion molecules and consequently cell adhesion (Dal *et al.,* 2003; Kaminski *et al.,* 2004), others show an increase in vasopermeability and a consequent rise in migration when low doses of NO are applied (Ajuebor *et al.,* 1998; Franco-Penteado *et al.,* 2001; Isenberg *et al.,* 2005). The relative concentration and intracellular location of NO release may be key to its function but a clear assessment is also complicated by its propensity to form a variety of oxidized derivatives (such as peroxynitrite), which often induce different (and also toxic) effects. During later stages of inflammation, lymphocyte migration is undoubtedly influenced by iNOS activity and the resultant proinflammatory gene expression (Kroncke, 2003). However, iNOS was not expressed within the time frame of our experiments and consequently not relevant to our observations. A promigratory role of NO was unambiguously demonstrated when DEA-NO or BAY-412272 was added to BAPTA-AM–pretreated ECs. This implies that the eNOS pathway could be targeted for novel anti-inflammatory therapies. However, in light of their pleiotropic functions during inflammation, eNOS or NO themselves probably do not constitute suitable targets. Other more unique components of the signaling pathway linking ICAM-1 to VEC phosphorylation, on which leukocyte migration appears to be exquisitely reliant, may prove more appropriate. Future investigation will focus

on the spatiotemporal requirements of ICAM-1–induced eNOS and VEC phosphorylation as well as the kinases and phosphatase involved. eNOS activation may lead to the rapid inactivation of a VEC tyrosine phosphatase by direct nitrosylation. However, the sensitivity of our system to the sGC inhibitor ODQ suggests a more complex network of regulation.

## ACKNOWLEDGMENTS

We thank Jeremy Pearson (King's College London, London, United Kingdom), Britta Engelhardt (University of Bern, Bern, Switzerland), and Evelyn Beraud for providing us with ICAM-1 CHO cells, mouse endothelioma cell lines, and antigen-activated T-cells, respectively. Adrian Hobbs kindly provided eNOS knockout mice. We thank Veronica Hollis, Miriam Palacios-Callender, and Salvador Moncada for help with direct NO measurements and helpful comments throughout this work and Reiner Haseloff for helpful comments throughout this work. This work was supported by a Program Grant from the Wellcome Trust (062403).

## REFERENCES

Abbott, N. J., Hughes, C. C., Revest, P. A., and Greenwood, J. (1992). Development and characterisation of a rat brain capillary endothelial culture: towards an in vitro blood-brain barrier. J. Cell Sci. *103*(Pt 1), 23–37.

Adamson, P., Etienne, S., Couraud, P. O., Calder, V., and Greenwood, J. (1999). Lymphocyte migration through brain endothelial cell monolayers involves signaling through endothelial ICAM-1 via a rho-dependent pathway. J. Immunol. *162*, 2964–2973.

Adamson, P., Wilbourn, B., Etienne-Manneville, S., Calder, V., Beraud, E., Milligan, G., Couraud, P. O., and Greenwood, J. (2002). Lymphocyte trafficking through the blood-brain barrier is dependent on endothelial cell heterotrimeric G-protein signaling. FASEB J. *16*, 1185–1194.

Ahluwalia, A., Foster, P., Scotland, R. S., McLean, P. G., Mathur, A., Perretti, M., Moncada, S., and Hobbs, A. J. (2004). Antiinflammatory activity of soluble guanylate cyclase: cGMP-dependent down-regulation of P-selectin expression and leukocyte recruitment. Proc. Natl. Acad. Sci USA *101*, 1386–1391.

Ajuebor, M. N., Virag, L., Flower, R. J., Perretti, M., and Szabo, C. (1998). Role of inducible nitric oxide synthase in the regulation of neutrophil migration in zymosan-induced inflammation. Immunology *95*, 625–630.

Allingham, M. J., van Buul, J. D., and Burridge, K. (2007). ICAM-1-mediated, Src- and Pyk2-dependent vascular endothelial cadherin tyrosine phosphorylation is required for leukocyte transendothelial migration. J. Immunol. *179*, 4053–4064.

Barreiro, O., Yanez-Mo, M., Serrador, J. M., Montoya, M. C., Vicente-Manzanares, M., Tejedor, R., Furthmayr, H., and Sanchez-Madrid, F. (2002). Dynamic interaction of VCAM-1 and ICAM-1 with moesin and ezrin in a novel endothelial docking structure for adherent leukocytes. J. Cell Biol. *157*, 1233–1245.

Boo, Y. C., Sorescu, G., Boyd, N., Shiojima, I., Walsh, K., Du, J., and Jo, H. (2002). Shear stress stimulates phosphorylation of endothelial nitric-oxide synthase at Ser1179 by Akt-independent mechanisms: role of protein kinase A. J. Biol. Chem. *277*, 3388–3396.

Busse, R., and Mulsch, A. (1990). Calcium-dependent nitric oxide synthesis in endothelial cytosol is mediated by calmodulin. FEBS Lett. *265*, 133–136.

Cambi, A., Joosten, B., Koopman, M., de, L. F., Beeren, I., Torensma, R., Fransen, J. A., Garcia-Parajo, M., van Leeuwen, F. N., and Figdor, C. G. (2006). Organization of the integrin LFA-1 in nanoclusters regulates its activity. Mol. Biol. Cell *17*, 4270–4281.

Carman, C. V., Jun, C. D., Salas, A., and Springer, T. A. (2003). Endothelial cells proactively form microvilli-like membrane projections upon intercellular adhesion molecule 1 engagement of leukocyte LFA-1. J. Immunol. *171*, 6135–6144.

Chen, Z. P., Mitchelhill, K. I., Michell, B. J., Stapleton, D., Rodriguez-Crespo, I., Witters, L. A., Power, D. A., Ortiz de Montellano, P. R., and Kemp, B. E. (1999). AMP-activated protein kinase phosphorylation of endothelial NO synthase. FEBS Lett. *443*, 285–289.

Cook-Mills, J. M. (2002). VCAM-1 signals during lymphocyte migration: role of reactive oxygen species. Mol. Immunol. *39*, 499–508.

Dal, S. D., Paron, J. A., de Oliveira, S. H., Ferreira, S. H., Silva, J. S., and Cunha, F. Q. (2003). Neutrophil migration in inflammation: nitric oxide inhibits rolling, adhesion and induces apoptosis. Nitric Oxide *9*, 153–164.

Deem, T. L., and Cook-Mills, J. M. (2004). Vascular cell adhesion molecule 1 (VCAM-1) activation of endothelial cell matrix metalloproteinases: role of reactive oxygen species. Blood *104*, 2385–2393.

Dejana, E., Orsenigo, F., and Lampugnani, M. G. (2008). The role of adherens junctions and VE-cadherin in the control of vascular permeability. J. Cell Sci. *121*, 2115–2122.

Dimmeler, S., Fleming, I., Fisslthaler, B., Hermann, C., Busse, R., and Zeiher, A. M. (1999). Activation of nitric oxide synthase in endothelial cells by Akt-dependent phosphorylation. Nature *399*, 601–605.

Engelhardt, B. (2006). Molecular mechanisms involved in T cell migration across the blood-brain barrier. J. Neural Transm. *113*, 477–485.

Etienne, S., Adamson, P., Greenwood, J., Strosberg, A. D., Cazaubon, S., and Couraud, P. O. (1998). ICAM-1 signaling pathways associated with Rho activation in microvascular brain endothelial cells. J. Immunol. *161*, 5755–5761.

Etienne-Manneville, S., Manneville, J. B., Adamson, P., Wilbourn, B., Greenwood, J., and Couraud, P. O. (2000). ICAM-1-coupled cytoskeletal rearrangements and transendothelial lymphocyte migration involve intracellular calcium signaling in brain endothelial cell lines. J. Immunol. *165*, 3375–3383.

Fisslthaler, B., Loot, A. E., Mohamed, A., Busse, R., and Fleming, I. (2008). Inhibition of endothelial nitric oxide synthase activity by proline-rich tyrosine kinase 2 in response to fluid shear stress and insulin. Circ. Res. *102*, 1520–1528.

Fleming, I., Schulz, C., Fichtlscherer, B., Kemp, B. E., Fisslthaler, B., and Busse, R. (2003). AMP-activated protein kinase (AMPK) regulates the insulin-induced activation of the nitric oxide synthase in human platelets. Thromb. Haemost. *90*, 863–871.

Franco-Penteado, C. F., DeSouza, I., Teixeira, S. A., Ribeiro-DaSilva, G., De, N. G., and Antunes, E. (2001). Role of nitric oxide on the increased vascular permeability and neutrophil accumulation induced by staphylococcal enterotoxin B into the mouse paw. Biochem. Pharmacol. *61*, 1305–1311.

Fulton, D., Gratton, J. P., McCabe, T. J., Fontana, J., Fujio, Y., Walsh, K., Franke, T. F., Papapetropoulos, A., and Sessa, W. C. (1999). Regulation of endothelium-derived nitric oxide production by the protein kinase Akt. Nature *399*, 597–601.

Fulton, D., Gratton, J. P., and Sessa, W. C. (2001). Post-translational control of endothelial nitric oxide synthase: why isn't calcium/calmodulin enough? J. Pharmacol. Exp. Ther. *299*, 818–824.

Fulton, D., Church, J. E., Ruan, L., Li, C., Sood, S. G., Kemp, B. E., Jennings, I. G., and Venema, R. C. (2005). Src kinase activates endothelial nitric-oxide synthase by phosphorylating Tyr-83. J. Biol. Chem. *280*, 35943–35952.

Gallis, B., *et al*. (1999). Identification of flow-dependent endothelial nitric-oxide synthase phosphorylation sites by mass spectrometry and regulation of phosphorylation and nitric oxide production by the phosphatidylinositol 3-kinase inhibitor LY294002. J. Biol. Chem. *274*, 30101–30108.

Greenwood, J., Wang, Y., and Calder, V. L. (1995). Lymphocyte adhesion and transendothelial migration in the central nervous system: the role of LFA-1, ICAM-1, VLA-4 and VCAM-1. Immunology *86*, 408–415.

Hardie, D. G., Hawley, S. A., and Scott, J. W. (2006). AMP-activated protein kinase–development of the energy sensor concept. J. Physiol. *574*, 7–15.

Harris, M. B., Ju, H., Venema, V. J., Liang, H., Zou, R., Michell, B. J., Chen, Z. P., Kemp, B. E., and Venema, R. C. (2001). Reciprocal phosphorylation and regulation of endothelial nitric-oxide synthase in response to bradykinin stimulation. J. Biol. Chem. *276*, 16587–16591.

Hill, M. M., Andjelkovic, M., Brazil, D. P., Ferrari, S., Fabbro, D., and Hemmings, B. A. (2001). Insulin-stimulated protein kinase B phosphorylation on Ser-473 is independent of its activity and occurs through a staurosporine-insensitive kinase. J. Biol. Chem. *276*, 25643–25646.

Hurley, R. L., Anderson, K. A., Franzone, J. M., Kemp, B. E., Means, A. R., and Witters, L. A. (2005). The $Ca^{2+}$/calmodulin-dependent protein kinase kinases are AMP-activated protein kinase kinases. J. Biol. Chem. *280*, 29060–29066.

Isenberg, J. S., Tabatabai, N., and Spinelli, H. M. (2005). Nitric oxide modulation of low-density mononuclear cell transendothelial migration. Microsurgery *25*, 452–456.

Kaminski, A., Pohl, C. B., Sponholz, C., Ma, N., Stamm, C., Vollmar, B., and Steinhoff, G. (2004). Up-regulation of endothelial nitric oxide synthase inhibits pulmonary leukocyte migration following lung ischemia-reperfusion in mice. Am. J. Pathol. *164*, 2241–2249.

Kroncke, K. D. (2003). Nitrosative stress and transcription. Biol. Chem. *384*, 1365–1377.

Ley, K., Lundgren, E., Berger, E., and Arfors, K. E. (1989). Shear-dependent inhibition of granulocyte adhesion to cultured endothelium by dextran sulfate. Blood *73*, 1324–1330.

Liao, F., Ali, J., Greene, T., and Muller, W. A. (1997). Soluble domain 1 of platelet-endothelial cell adhesion molecule (PECAM) is sufficient to block transendothelial migration in vitro and in vivo. J. Exp. Med. *185*, 1349–1357.

Lyck, R., Reiss, Y., Gerwin, N., Greenwood, J., Adamson, P., and Engelhardt, B. (2003). T-cell interaction with ICAM-1/ICAM-2 double-deficient brain endothelium in vitro: the cytoplasmic tail of endothelial ICAM-1 is necessary for transendothelial migration of T cells. Blood *102*, 3675–3683.

Marletta, M. A. (2001). Another activation switch for endothelial nitric oxide synthase: why does it have to be so complicated? Trends Biochem. Sci. *26*, 519–521.

Matheny, H. E., Deem, T. L., and Cook-Mills, J. M. (2000). Lymphocyte migration through monolayers of endothelial cell lines involves VCAM-1 signaling via endothelial cell NADPH oxidase. J. Immunol. *164*, 6550–6559.

Montagnani, M., Chen, H., Barr, V. A., and Quon, M. J. (2001). Insulin-stimulated activation of eNOS is independent of $Ca^{2+}$ but requires phosphorylation by Akt at Ser(1179). J. Biol. Chem. *276*, 30392–30398.

Morrow, V. A., Foufelle, F., Connell, J. M., Petrie, J. R., Gould, G. W., and Salt, I. P. (2003). Direct activation of AMP-activated protein kinase stimulates nitric-oxide synthesis in human aortic endothelial cells. J. Biol. Chem. *278*, 31629–31639.

Motley, E. D., Eguchi, K., Patterson, M. M., Palmer, P. D., Suzuki, H., and Eguchi, S. (2007). Mechanism of endothelial nitric oxide synthase phosphorylation and activation by thrombin. Hypertension *49*, 577–583.

Murakami, H., *et al.* (2006). Fenofibrate activates AMPK and increases eNOS phosphorylation in HUVEC. Biochem. Biophys. Res. Commun. *341*, 973–978.

Nagata, D., Mogi, M., and Walsh, K. (2003). AMP-activated protein kinase (AMPK) signaling in endothelial cells is essential for angiogenesis in response to hypoxic stress. J. Biol. Chem. *278*, 31000–31006.

Perez, O. D., Kinoshita, S., Hitoshi, Y., Payan, D. G., Kitamura, T., Nolan, G. P., and Lorens, J. B. (2002). Activation of the PKB/AKT pathway by ICAM-2. Immunity *16*, 51–65.

Pober, J. S., and Sessa, W. C. (2007). Evolving functions of endothelial cells in inflammation. Nat. Rev. Immunol. *7*, 803–815.

Ren, X. D., Kiosses, W. B., and Schwartz, M. A. (1999). Regulation of the small GTP-binding protein Rho by cell adhesion and the cytoskeleton. EMBO J. *18*, 578–585.

Romero, I. A., Radewicz, K., Jubin, E., Michel, C. C., Greenwood, J., Couraud, P. O., and Adamson, P. (2003). Changes in cytoskeletal and tight junctional proteins correlate with decreased permeability induced by dexamethasone in cultured rat brain endothelial cells. Neurosci. Lett. *344*, 112–116.

Six, I., Kureishi, Y., Luo, Z., and Walsh, K. (2002). Akt signaling mediates VEGF/VPF vascular permeability in vivo. FEBS Lett. *532*, 67–69.

Stahmann, N., Woods, A., Carling, D., and Heller, R. (2006). Thrombin activates AMP-activated protein kinase in endothelial cells via a pathway involving $Ca^{2+}$/calmodulin-dependent protein kinase kinase beta. Mol. Cell. Biol. *26*, 5933–5945.

Turowski, P., Adamson, P., and Greenwood, J. (2005). Pharmacological targeting of ICAM-1 signaling in brain endothelial cells: potential for treating neuroinflammation. Cell Mol. Neurobiol. *25*, 153–170.

Turowski, P., Adamson, P., Sathia, J., Zhang, J. J., Moss, S. E., Aylward, G. W., Hayes, M. J., Kanuga, N., and Greenwood, J. (2004). Basement membrane-dependent modification of phenotype and gene expression in human retinal pigment epithelial ARPE-19 cells. Invest. Ophthalmol. Vis. Sci. *45*, 2786–2794.

Turowski, P. *et al.* (2008). Phosphorylation of vascular endothelial cadherin controls lymphocyte emigration. J. Cell Sci. *121*, 29–37.

van Hinsbergh, V., and van Nieuw Amerongen, G. P. (2002). Intracellular signalling involved in modulating human endothelial barrier function. J. Anat. *200*, 549–560.

Wang, Q., Pfeiffer, G. R., and Gaarde, W. A. (2003). Activation of SRC tyrosine kinases in response to ICAM-1 ligation in pulmonary microvascular endothelial cells. J. Biol. Chem. *278*, 47731–47743.

Zhou, G., *et al.* (2001). Role of AMP-activated protein kinase in mechanism of metformin action. J. Clin. Invest. *108*, 1167–1174.